Specific heat of $Na_{0.3}CoO_2 \cdot 1.3H_2O$: Two energy gaps, nonmagnetic pair breaking, strong fluctuations in the superconducting state, and effects of sample age

N. Oeschler,[1] R. A. Fisher,[1] N. E. Phillips,[1] J. E. Gordon,[2] M.-L. Foo,[3] and R. J. Cava[3]
[1]*Lawrence Berkeley National Laboratory and Department of Chemistry, University of California, Berkeley, California 94720, USA*
[2]*Physics Department, Amherst College, Amherst, Massachusetts 01002, USA*
[3]*Department of Chemistry, Princeton University, Princeton, New Jersey 08544, USA*
(Received 7 May 2008; published 27 August 2008)

The specific heat of three samples of $Na_{0.3}CoO_2 \cdot 1.3H_2O$ shows an evolution of the superconductivity and its eventual disappearance with increasing sample age. The specific heat of two superconducting samples is characteristic of a superconductor with two energy gaps, which implies contributions of two electron bands to the Fermi surface. The changes in the specific heat are associated with a nonmagnetic pair-breaking action that progresses with sample age and acts preferentially in the band with the smaller gap to produce an increasing "residual" electron density of states and a shift in the relative contributions of the bands to the superconducting condensate. For the nonsuperconducting sample the pair breaking has weakened the superconducting-state electron pairing to the point that it has given way to a competing order. The similarity of the time scale for these changes to that recently reported for the formation of O vacancies suggests a relation between the two effects and the identification of the O vacancies as the pair-breaking scattering centers. Together, these effects provide an understanding of the strong sample dependence of the properties of this material. They also suggest an unusual competition between two effects of the O vacancies: enhancement of the superconductivity at low concentrations by adjusting the carrier concentration and destruction of the superconductivity at high concentrations by pair breaking. Comparison of the coefficient of the normal-state conduction-electron specific heat, $\gamma_n = 16.1$ mJ K^{-2} mol^{-1}, with band-structure calculations supports the existence of the controversial e_g' hole pockets in the Fermi surface, in addition to the well established a_{1g} surface. The onset of the transition to the vortex state is independent of magnetic field, suggesting the presence of unusually strong fluctuation effects. The specific-heat results and their implications for band structure and symmetry of the superconducting-state order parameter are compared with other experimental and theoretical results.

DOI: 10.1103/PhysRevB.78.054528 PACS number(s): 74.25.Bt

I. INTRODUCTION

The discovery of superconductivity in the cuprates,[1] with critical temperatures (T_c) as high as 133 K,[2] raised the question of whether high-T_c superconductivity might be found in similar systems with other ions replacing Cu. Although Co was recognized as an interesting candidate almost immediately, the very fragile superconductivity of $Na_{0.35}CoO_2 \cdot 1.3H_2O$, with $T_c \sim 4.5$ K, was not discovered until 2003.[3] $Na_{0.3}CoO_2 \cdot 1.3H_2O$ displays most of the structural and electronic features thought to be important for the superconductivity in the cuprates—strong two-dimensional (2D) character, proximity to a magnetically ordered nonmetallic state, and electron spin 1/2—and T_c has the same unusual "dome-shaped" dependence on doping. There is, however, one interesting difference: in the cuprates Cu ions in an approximately *square* array are ordered antiferromagnetically, and spin fluctuations are thought to play a role in the electron pairing; in $Na_{0.3}CoO_2 \cdot 1.3H_2O$ Co ions in a *triangular* array are magnetically frustrated, which may affect the superconductivity. A considerable body of theoretical work suggests that the superconductivity is different from that of the cuprates but still "unconventional." However, there is no consensus on the nature of the order parameter (OP), which is the basis for comparison of theoretical models with experimental results. A major problem is uncertainty about the nature of the Fermi surface, whether it consists of the zone-centered a_{1g} sheet alone or whether it also includes six small e_g' pockets, the existence of which is crucial to some of the models. On the experimental side the situation is also confused: the sample-to-sample variation of the properties has prevented an unambiguous determination of the intrinsic properties that would give information on the symmetry of the OP. Mazin and Johannes[4] made a systematic comparison of experimental results with the possible OPs. They have suggested that the superconductivity may be unique, but they have recognized that "experimental reports are often contradictory and solid evidence for any particular pairing state remains lacking," and they have noted ambiguity in the interpretation of the specific heat in particular.

The specific heat gives information on the symmetry of the OP, specifically on the existence of nodes in the energy gap. A number of specific-heat measurements have been reported,[5–16] but in many cases the interpretation of the results is limited by contributions from paramagnetic centers, lack of data at sufficiently low temperatures and in magnetic fields, or possible experimental error. The more fundamental problem, however, is that the results that are relatively free of these shortcomings show a strong sample dependence. Measurements of other properties that give information about the OP, by NMR, nuclear quadrupole resonance (NQR), and muon spin relaxation (μSR), have shown a similar sample dependence. The superconducting-state specific heat includes a sample-dependent contribution associated with the superconducting condensate and a normal-state-like contribution that corresponds to a "residual" electron density

 ©2008 The American Physical Society

of states (DOS), which is also sample dependent. The latter has generally been attributed to incomplete transitions to the superconducting state and the presence of normal material, but a similar residual DOS seen in measurements of the nuclear-spin-relaxation time (T_1) has been attributed to pair breaking.

We have measured the specific heat of three samples of $Na_{0.3}CoO_2 \cdot 1.3H_2O$ that had no significant concentrations of paramagnetic centers. The measurements extended to the temperature region in which features associated with energy-gap nodes should be evident. The samples differed in sample age (storage time at ambient temperature before the measurements): approximately 3, 5, and 40 days for samples 2, 3, and 1, respectively (numbered in the order in which the measurements were made). Shortly after preparation, sample 1 was superconducting, as shown by susceptibility measurements, but the specific-heat measurements showed only a weakly field-dependent anomaly near 7 K and no superconductivity. The disappearance of the superconductivity was confirmed by subsequent susceptibility measurements. The 7 K specific-heat anomaly will be described and compared with a theoretical prediction of charge-density wave (CDW) ordering in another publication.[17] The measurements on samples 2 and 3 have been described in several preliminary reports,[15,16] but a more complete description of the results, their analysis, and their implications is given here. These samples showed superconducting transitions at essentially the same temperature, $T_c \sim 4.5$ K, but substantial differences in the nature of the superconducting condensate and in the residual DOS. The differences in the specific heat of samples 2 and 3 show that the normal-material model for the residual DOS invoked for the cuprates is not applicable to $Na_{0.3}CoO_2 \cdot 1.3H_2O$. Instead, the residual DOS is a consequence of pair breaking, which increases with increasing sample age and produces the change in the superconducting condensate. The specific-heat results are consistent with other recent evidence that the superconducting forms of this material are thermodynamically unstable and the superconductivity evolves with sample age on a time scale of several days[18,19] and ultimately disappears.[19] Changes in T_c are accompanied by changes in the residual DOS,[18] Co oxidation state, crystal structure, and concentration of O vacancies.[19] In this context, samples 2, 3, and 1 correspond to different stages in a progression through a series of closely related superconducting materials that terminates in a nonsuperconducting material. Since the instability of the O stoichiometry seems to be an *inherent* property of the superconducting materials, the measured specific heats *are*, in this sense, intrinsic properties, the intrinsic properties of slightly different unstable materials characterized by different O stoichiometries. The specific-heat results provide an understanding of the "sample dependence" of the properties at a phenomenological level and show that the effects of pair breaking must be taken into account in any comparison of experimental results with theoretical predictions. They also provide evidence supporting the existence of a second sheet of the Fermi surface, the e_g' pockets, which are predicted in some band-structure calculations.

Following a brief description of the sample preparation and specific-heat measurements in Sec. II, the analysis of the specific heat into its component contributions and the relevant notation are described in Sec. III. The specific-heat results and the separation of the electron contribution are presented in Sec. IV; the argument that the residual DOS is associated with pair breaking in Sec. V; and the evidence for two gaps and the (ambiguous) evidence for line nodes in the small gap in Sec. VI. Section VII is a phenomenological interpretation of the specific heat and the effects of sample age based in part on a comparison with the recently recognized[19] occurrence of O vacancies. Our specific-heat results are compared with others in Sec. VIII, where it is also shown that the combinations of features seen in our samples are not unique but are similar to those seen in several other samples, supporting our conclusion that the sample dependence is not a consequence of random unrelated deficiencies in "sample quality." The specific-heat results are compared with theoretical and experimental band-structure results in Sec. IX, implications of experimental results for symmetry of the order parameter are discussed in Sec. X, and the conclusions are summarized in Sec. X.

II. SAMPLES: SPECIFIC-HEAT MEASUREMENTS

Polycrystalline samples of $Na_{0.3}CoO_2 \cdot 1.3H_2O$, with the Na content at the optimum value for high T_c, were prepared by deintercalating Na from $Na_{0.75}CoO_2$ with Br_2 in acetonitrile at 40 times the stoichiometric concentration.[20] X-ray diffraction measurements showed the superconducting bilayer hydrate material and no detectable level of other phases. After drying, samples 1–3 were kept at ambient temperature in a 100% relative humidity environment for approximately 40, 3, and 5 days, respectively. The samples were cooled to liquid nitrogen temperatures before evacuating the surrounding space to eliminate the possibility of dehydration. Sample 2 was kept near 4 K for approximately 30 days and showed no change in specific heat in that period.

The specific-heat measurements were made by a heat-pulse technique, which minimizes the possibility of errors associated with internal equilibrium times that may not be recognized in measurements by the relaxation technique (see Sec. VIII). The measurements extended over the temperature (T) intervals 0.85–32 K for sample 2 and 0.34–14 K for sample 3. For sample 2 they included measurements in magnetic fields (H) to $\mu_0 H = 9$ T. Small amounts of water, in excess of the water of hydration, were added to the samples to enhance thermal contact and reduce equilibrium times. The corrections for the heat capacity of the excess water were based on published data.[21] Errors in the heat capacity of the water used in the corrections would affect the derived values of the lattice contribution to the specific heat, but not the electron contribution, which is the quantity of most interest.

III. SPECIFIC-HEAT COMPONENTS: NOTATION—OVERVIEW OF DATA ANALYSIS

A. Contributions to the specific heat

The specific heat (C) of samples 2 and 3 includes four components: the electron contribution (C_e), the lattice con-

tribution (C_{lat}), a "hyperfine" contribution (C_{hyp}), which is associated with the interaction of nuclear magnetic moments with an applied field, and a "magnetic" contribution (C_{mag}), which is associated with paramagnetic centers. An applied magnetic field is indicated by H or a numerical value in parentheses, e.g., $C(H)$ for C in a field H and $C(9\ \text{T})$ for C in a field $\mu_0 H = 9$ T. The normal-state electron contribution is $C_{en} = \gamma_n T$. For $T \leq 12$ K, the lattice contribution is represented by the first three terms in the harmonic-lattice approximation, $C_{lat} = B_3 T^3 + B_5 T^5 + B_7 T^7$. For the ranges of T and H of interest, C_{hyp} is proportional to $(H/T)^2$. For sample 2 there is a low concentration of paramagnetic centers, which are ordered by internal interactions in low applied fields, but by the applied field in higher applied fields. In low fields they contribute a T^{-2} term to C_{mag} that is observable near 1 K in the superconducting and vortex states, in which the other contributions to C are small. In higher fields C_{mag} would be a Schottky function, with an argument proportional to H/T, but it would occur at higher T where it is too small to be observable in the presence of the larger contributions from C_e and C_{lat}. The coefficients of the terms in C_{lat} and γ_n were obtained by fitting the normal-state data with the expression for $C_{en} + C_{lat}$ after subtracting C_{hyp}, which was determined by a separate fit to the lowest-T data. The electron contributions in the superconducting and vortex states, $C_{es} = C_e(0)$ for $T \leq T_c$ and $C_{ev}(H) = C_e(H)$ for $T \leq T_c$ and $0 < H < H_{c2}$, were obtained by subtracting C_{lat}, C_{mag}, and C_{hyp} from C.

B. Electron contributions "normalized to 1 mol of superconducting condensate," C_e'

All specific-heat measurements on superconducting samples of this material that permit reasonably unambiguous extrapolations to 0 K show a normal-state-like contribution to $C_e(0)$ which is represented in the following by $\gamma_r T$. In reports of other measurements and in a preliminary report[15] on our sample 2, it was attributed to an incomplete transition to the superconducting-state and volume fractions of normal and superconducting material γ_r/γ_n and $(\gamma_n - \gamma_r)/\gamma_n$, respectively. On that basis, the specific heat is the sum of separate contributions of the superconducting and normal phases, $C_e(H)$ for 1 mol of superconducting material is $C_e'(H) = [C_e(H) - \gamma_r T)]\gamma_n/(\gamma_n - \gamma_r)$, and for the superconducting state, $C_{es}' = [(C_{es} - \gamma_r T)]\gamma_n/(\gamma_n - \gamma_r)$. Many of the specific-heat results have been reported in that form. However, the $\gamma_r T$ contribution is actually a consequence of pair breaking, not the presence of normal material (see Sec. V), and in principle the specific heat is not the sum of separate contributions of broken pairs and the superconducting condensate. Nevertheless, as discussed in Sec. V, $C_e'(H)$ and C_{es}' can be expected to be reasonable and useful approximations to the specific heat of 1 mol of superconducting condensate, and they are used in the following for that purpose. In figures, they are also used to emphasize the difference in the superconducting condensates in samples 2 and 3 and to facilitate comparisons with BCS theory, other superconductors that have no pair breaking, and other samples of this material for which the results have been reported in that form. The same notation is used generally for other quantities normalized to 1 mol of superconducting condensate in this way, e.g., for $\gamma_v(H)$, the coefficient of the T-proportional term in $C_{ev}(H)$, $\gamma_v'(H) = [\gamma_v(H) - \gamma_r]\gamma_n/(\gamma_n - \gamma_r)$.

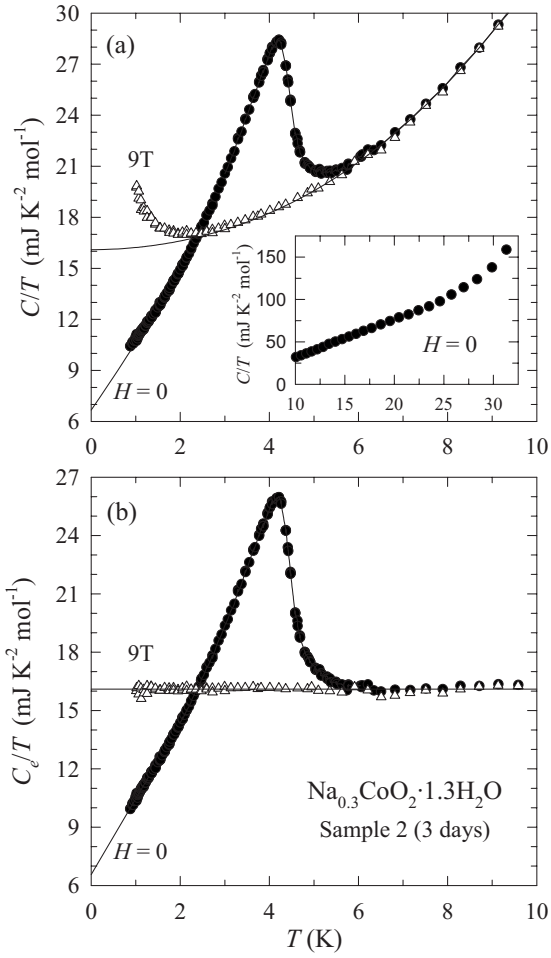

FIG. 1. Specific heat of sample 2. (a) The total specific heat. The curved line associated with the $H=0$ points in the main panel represents the lattice plus electron contributions. (b) The electron contributions to the normal and superconducting states are derived as described in the text. (These data were also published in Ref. 16.)

IV. SPECIFIC-HEAT RESULTS: ELECTRON CONTRIBUTION

A. Normal- and superconducting-state specific heat of sample 2

The general nature of the results is illustrated by Figs. 1(a) and 1(b), respectively, $C(0)$ and $C(9\ \text{T})$ and $C_e(0)$ and $C_e(9\ \text{T})$, which show the specific-heat anomaly at T_c and the absence of other transitions below 30 K. (These data were also published in Ref. 16.) In particular, there is no trace of the anomaly associated with the 7 K transition in sample 1. A T^{-2} term, the low-T "upturn" in the 9 T data in Fig. 1(a), and similar terms in 3, 5, and 7 T are in good agreement with calculated hyperfine contributions, C_{hyp}, *for those nuclei in the sample*. Apparently the protons in the excess water do not relax on the time scale of the measurements and do not contribute. In 9 T there is no indication of the transition to the

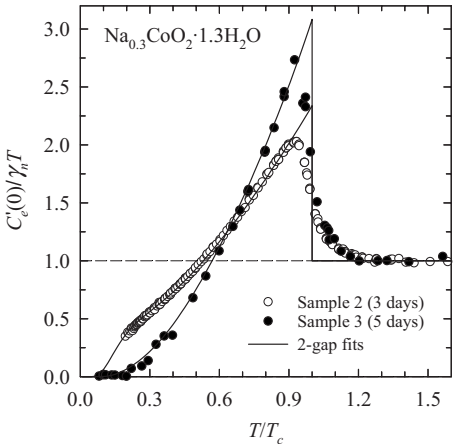

FIG. 2. The zero-field electron specific heat of samples 2 and 3, normalized to 1 mol of superconducting condensate (see Sec. III B). For $T \leq T_c$, $C'_e(0) = C'_{es}$. The entropy-conserving constructions at T_c give the values of T_c and $\Delta C'_{es}(T_c)/\gamma_n T_c$.

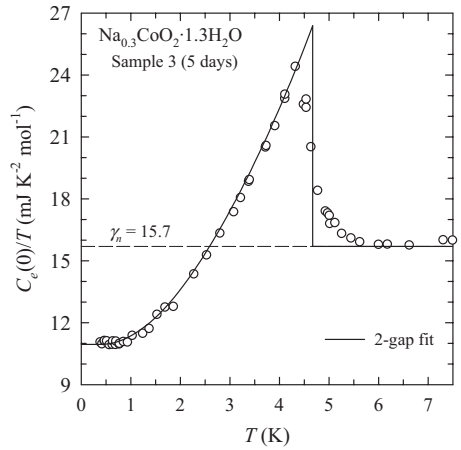

FIG. 3. The zero-field electron specific heat of sample 3. For $T \leq T_c$, $C_e(0) = C_{es}$.

vortex state that is apparent for all other fields, including 7 T (see Fig. 4). This suggests an upper limit for the anisotropic $H_{c2}(0)$, $\mu_0 H_{c2}(0) = 9$ T. After subtraction of the T^{-2} term, $C(9\ \text{T})$ to 12 K was combined with $C(0)$ from 6 to 12 K and fitted as $C = C_{en} + C_{lat} = \gamma_n T + B_3 T^3 + B_5 T^5 + B_7 T^7$. The fit gave $\gamma_n = 16.1$ mJ K^{-2} mol^{-1} and $B_3 = 0.126$ mJ K^{-4} mol^{-1}.

For $\mu_0 H \leq 1$ T, small T^{-2} terms—e.g., an upturn in the $H=0$ data—which is barely perceptible in Fig. 1(a), are evidence of a contribution, C_{mag}, associated with paramagnetic centers at a concentration of $\sim 10^{-3}$ mol/mol sample, which make no observable contribution to $C(H)$ at higher T, as shown in Figs. 1(a) and 4. The conduction-electron contribution, $C_e(H) = C(H) - C_{lat} - C_{hyp}(H) - C_{mag}(H)$, is shown in Fig. 1(b). Below 2 K, $C_{es} = C_e(0)$ is the sum of T and T^2 terms. C_{es}/T is linear in T, and extrapolation to $T=0$ gives a 6.5 K entropy that agrees with the values obtained from the data in magnetic fields (to within +1.5% for 9 T and $\pm 0.5\%$ for other fields). The extrapolation gives a nonzero intercept, $\gamma_r = 6.41$ mJ K^{-2} mol^{-1}, a normal-state-like "residual γ" that is a measure of the residual DOS. An entropy-conserving construction on $C'_e(0)$, shown in Fig. 2, gives $T_c = 4.52$ K and $\Delta C'_{es}(T_c)/\gamma_n T_c = 1.38$ for the discontinuity in C_{es} at T_c, normalized to 1 mol of superconducting condensate and to the normal-state specific heat at T_c.

The T^2 term in C_{es} is expected for line nodes in the energy gap and is usually taken as evidence of their existence. It has also been identified by Yang *et al.*[13] in another sample, referred to as sample A in the following, which is similar to sample 2 in other respects as well. However, as discussed in Sec. VI, C_{es} can also be represented as the sum of contributions from two electron bands with different energy gaps, without a T^2 term. The absence of a T^2 term in C'_{es} for sample 3 (see below) led to a re-examination of the data for sample 2 and the recognition that the T^2 term, *in the temperature interval in which it is observed*, could be a coincidental result of the superposition of the contributions of the two bands and not necessarily evidence of nodes.

B. Normal- and superconducting-state specific heat of sample 3

For sample 3 there is no evidence of paramagnetic impurities and as for sample 2, no evidence of the 7 K anomaly. Fitting $C(0)$ for $6 \leq T \leq 12$ K with the expressions used for sample 2 and with the constraint that the normal-state and zero-field entropies be equal at 6.5 K gave $\gamma_n = 15.7$ mJ K^{-2} mol^{-1}. There is no evidence of a T^2 term in $C(0)$: the lowest-T data can be fitted as the sum of an exponential term, as expected for a "fully gapped" superconductor, and $\gamma_r T$, with $\gamma_r = 11.0$ mJ K^{-2} mol^{-1}. However, as discussed in Sec. VI, a T^2 term associated with nodes could be obscured by the $\gamma_r T$ term, and C_{es} for this sample is also consistent with two gaps. $C_e(0)$ is shown in Fig. 3. An entropy-conserving construction on $C'_e(0)$, shown in Fig. 2, gives $T_c = 4.65$ K, and $\Delta C'_{es}(T_c)/\gamma_n T_c = 2.08$.

C. Vortex-state specific heat of sample 2

Vortex-state data for sample 2 are shown in Fig. 4 as $C'_e(H)$. The temperature of the onset of the transition to the mixed state is independent of H. This effect is expected for strong fluctuations, but it is unusually large for a superconductor with such a low T_c. The same effect was observed by Yang *et al.*[13] in sample A. It was also observed and attributed to fluctuations, in another sample, referred to as sample B in the following, which was studied by Yang *et al.*[12]

For $H \neq 0$, $C'_e(H)/T$ is linear in T for appreciable intervals in T, just as it is for $H=0$. Values of $\gamma_v(H)$, the coefficient of the vortex-state T-proportional contribution to $C_e(H)$, obtained by analysis of the data in the intervals in which the linearity is best defined, are shown as $\gamma'_v(H)$ in the inset of Fig. 4 (see also Fig. 8) and discussed in Sec. VI. The accuracy of the values of $\gamma'_v(H)$ is limited by the precision of the data and the narrow intervals of T in which the linearity is defined, and the minimal scatter about smooth curves displayed in Figs. 4 and 8 is to some degree fortuitous. Their accuracy also depends on the assumption that the linearity extends to 0 K. The relation of the values of $\gamma'_v(H)$ for $\mu_0 H \leq 7$ T to the normal state γ_n plotted at 9 T shows that

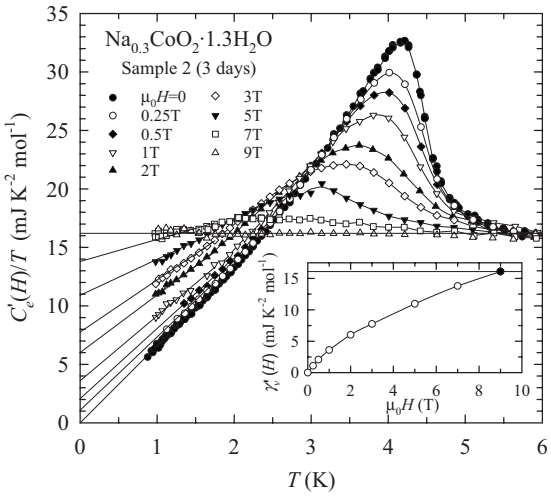

FIG. 4. The vortex-state electron specific heat of sample 2 (main panel) and $\gamma_v'(H)$ vs H (inset), both normalized to 1 mol of superconducting condensate (see Sec. III B). The open circles in the inset, for $\mu_0H \leq 7$ T, were obtained by the extrapolations of the vortex-state data described in the text; the solid circle at $\mu_0H = 9$ T is the normal-state value, γ_n (see Sec. IV A).

$\mu_0H_{c2}(0)$ is not significantly different from the upper limit of 9 T deduced from the H dependence of the specific-heat anomaly at T_c. Sample-dependent pair breaking could produce a sample-to-sample variation of $H_{c2}(0)$, but several measurements[10,22,23] of H_{c2} for H parallel to the *ab* plane suggest similar values.

V. RESIDUAL DENSITY OF STATES: PAIR BREAKING

Specific-heat measurements on the cuprate superconductors, particularly early measurements on poor-quality samples, showed the existence of samples with essentially the same T_c but different values of $\Delta C_e(T_c)$, which decreased with increasing γ_r. These results were interpreted in terms of normal material on the scale of the coherence length, which is of the order of a lattice parameter in the cuprates, with the superconductivity suppressed by atomic-scale defects or inhomogeneity. In the context of penetration-depth measurements, which suggested a similar interpretation, the term "Swiss cheese" was used to described the mixture of normal and superconducting regions.[24] In this model different samples are different mixtures of the normal phase and the *same* superconducting phase, and the electron specific heat for 1 mol of superconducting material is $C_e'(H) = [C_e(H) - \gamma_r T)]\gamma_n/(\gamma_n - \gamma_r)$. There are samples of $Na_{0.3}CoO_2 \cdot 1.3H_2O$ with essentially the same T_c, ~4.5 K, but substantially different values of γ_r. By analogy with the early measurements on the cuprates, these results have been interpreted quite generally in terms of the presence of normal material. However, the longer coherence length makes that model less plausible for $Na_{0.3}CoO_2 \cdot 1.3H_2O$. Furthermore, as shown in Fig. 2, C_{es}' is not the same for samples 2 and 3, the superconductivity is *different*, and the normal-material model developed for the cuprates is not applicable.

The other mechanism for producing a residual DOS, which is also known in the cuprates, is pair breaking by scattering centers. It is usually accompanied by a reduction in T_c but that can be small in the case of resonant scattering.[25–27] In addition, there are clearly competing effects that influence T_c in different ways in $Na_{0.3}CoO_2 \cdot 1.3H_2O$ (see Sec. VII). The sample-dependent residual DOS seen in measurements of the spin-lattice relaxation time (T_1) has, also quite generally, been attributed to pair breaking (see, e.g., Refs. 28 and 29). It is possible to fit the time dependence of the relaxation reported in Ref. 29 at one temperature as a superposition of contributions from normal and superconducting regions, but the same mixture of normal and superconducting regions would not fit the data at other temperatures. Furthermore, the same nuclei see both the transition at T_c and the residual DOS, ruling out a two-phase interpretation.

The specific-heat results alone do not rule out the presence of normal material as the origin of the residual DOS. In principle, the different values of γ_r for samples 2 and 3 could be unrelated to the difference in the superconductivity but that would require independent explanations for the suppression of the superconductivity and its sample-to-sample variation. The T_1 results, on the other hand, cannot be understood on the basis of a sample-dependent mixture of two phases and require an interpretation in terms of pair breaking. With this interpretation of γ_r, C_{es}' would be only an approximation to C_{es} for the "pure" superconducting state, but there is reason to expect it to show the main features. The dependences of T_1 and C_{es} on the DOS are closely related, and the T_1 data (see, e.g., Refs. 28 and 29) show a fairly sharp transition from the T dependence associated with the residual DOS at low T to that characteristic of the pure superconducting state at higher T. Furthermore, calculations for a particular example of pair breaking[30] that account for the behavior of T_1 give a DOS that is qualitatively consistent with C_{es}'. In addition, for classic gapless superconductors, e.g., Th-Gd alloys, C_{es} is, to a good approximation, the sum of $\gamma_r T$ and BCS-type terms.[31] With these results as justification, we take $C_{es} - \gamma_r T = (1 - \gamma_r/\gamma_n)C_{es}'$ as an approximation to the contribution of the superconducting condensate to C_{es} and C_{es}' as an approximation to C_{es} in the absence of pair breaking.

VI. EVIDENCE FOR TWO GAPS—EVIDENCE FOR GAP NODES

For sample 2, C_{es}' shows unusual deviations from BCS theory, which, however, are strikingly similar to those for MgB_2 (see Fig. 5). The deviations for MgB_2 were without precedent at the time of the discovery of its superconductivity, but it is now well established that they are a consequence of additive contributions to C_{es} from two electron bands with different energy gaps in the superconducting state (see, e.g., Ref. 32). The smaller gap produces the positive deviations from BCS at low temperature and the larger gap produces the strong-coupling character of C_{es} near T_c, the positive curvature in Fig. 5. The MgB_2 data are accurately represented by a two-gap fit that gives the DOS and the gap amplitude for each band in good agreement with both theoretical and other experimental results.[32] More recently, somewhat similar deviations from BCS theory[33] for Sr_2RuO_4 have been

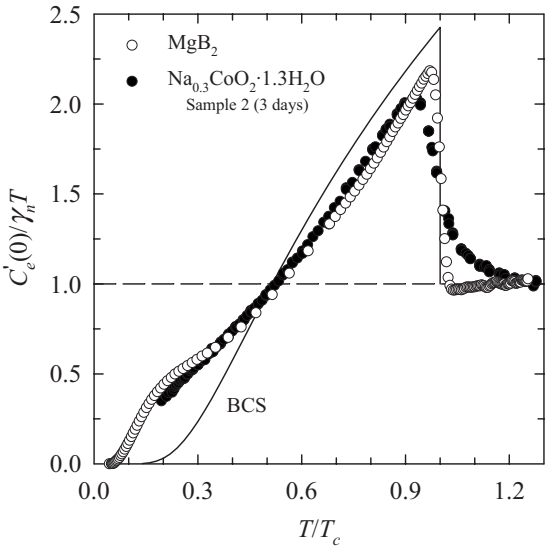

FIG. 5. The zero-field electron specific heat of sample 2, normalized to 1 mol of superconducting condensate (see Sec. III B), compared with BCS theory and with the electron specific heat of MgB_2. For $T \leq T_c$, $C'_e(0) = C'_{es}$.

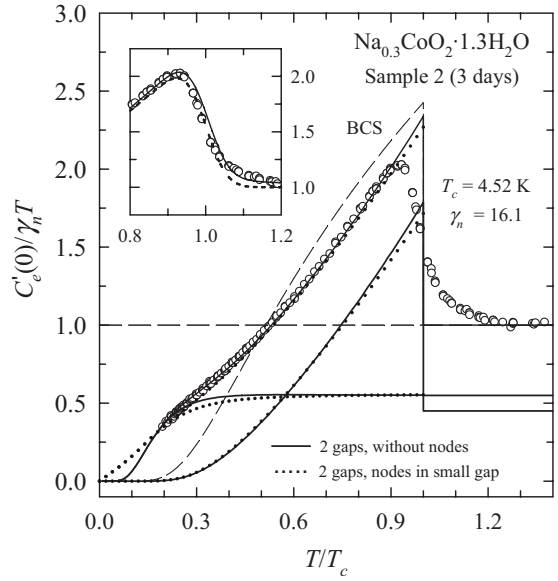

FIG. 6. The zero-field electron specific heat of sample 2, normalized to 1 mol of superconducting condensate (see Sec. III B), compared with BCS theory and two two-gap fits. For $T \leq T_c$, $C'_e(0) = C'_{es}$. Inset: Gaussian fits to the zero-field data near T_c, with (solid line) and without (dotted line) a fluctuation contribution.

shown[33,34] to be associated with contributions from three bands with different gaps and line nodes in one of the gaps. Among all other superconductors, deviations from BCS theory comparable in magnitude and T dependence to those shown by $Na_{0.3}CoO_2 \cdot 1.3H_2O$ are unique to these two cases, in both of which they are known to be associated with multigap structure. These similarities, particularly to MgB_2, are evidence of the presence of two gaps, one of which is substantially smaller in relation to T_c than given by BCS theory.

For both samples 2 and 3 C_{es} is well represented by two-gap fits similar to those made for MgB_2. In these fits C_{es} is the sum of *three* contributions: the $\gamma_r T$ term associated with the broken pairs and the contributions of the two components of the superconducting condensate derived from the two electron bands, $i=1,2$. The temperature dependences of the superconducting-condensate contributions are those given by the α model,[35] in which the BCS temperature dependence of the *gap* is assumed, but the 0 K amplitude, $\Delta(0)$, is an adjustable parameter represented by $\alpha \equiv \Delta(0)/k_B T_c$. (In the weak-coupling limit of BCS theory $\alpha = 1.764$.) The amplitudes of these contributions are proportional to an "effective γ," γ_{is}, which is a measure of the DOS that the band contributes to the superconducting condensate. They are constrained by the requirement that the two contributions add to $C_{es} - \gamma_r T$, which is equivalent to the requirement that $\gamma_{1s} + \gamma_{2s} = \gamma_n - \gamma_r$. The fits introduce three adjustable parameters, α_1, α_2, and γ_{1s}/γ_{2s}, and give the values of α_1, α_2, and the fractions of the *total* normal-state DOS that the bands contribute to the superconducting condensate, γ_{1s}/γ_n, and γ_{2s}/γ_n. In the following, the subscripts 1 and 2 identify parameters associated with the "large-gap" and "small-gap" bands, respectively. Several two-gap fits for sample 2 are shown in Fig. 6, where they are represented by C'_{es}, i.e., normalized to 1 mol of superconducting condensate (see Sec. III B). The dotted curves represent a fit based on the assumption of line nodes in the small gap, with $\alpha_1 = 2.15$, $\alpha_2 = 1.00$, $\gamma_{1s}/\gamma_n = 0.33$, and $\gamma_{2s}/\gamma_n = 0.27$. The small-gap contribution was calculated using the BCS temperature dependence for the gap, as in the α model, but allowing for the presence of line nodes to reproduce the T^2 behavior observed for $0.2 \leq T/T_c \leq 0.4$ and extend it to 0 K. The absence of evidence for nodes in sample 3 led to an alternative interpretation of the sample 2 data based on a fully gapped model. The solid curves in Fig. 6 represent a two-gap fit without nodes and $\alpha_1 = 2.20$, $\alpha_2 = 0.70$, $\gamma_{1s}/\gamma_n = 0.33$, and $\gamma_{2s}/\gamma_n = 0.27$. With these parameters, the T^2 dependence is reproduced, in the T interval in which it is observed, without nodes. (The extrapolation of this fit to 0 K gives a 6.5 K entropy that is $\sim 0.5\%$ lower than that given by the T^2 extrapolation. Given the $\sim 1\%$ entropy discrepancies in data for different fields described in Sec. IV A, this difference is too small to suggest a choice of one fit over the other.) The two-gap fits are based on an assumed discontinuity in the gap amplitude. Even with a comparable spread in gap amplitude, a single anisotropic gap that varied slowly over the Fermi surface, as may be the case for $NbSe_2$ (see Ref. 36), would smear out the relatively sharp change in sign of the deviations from the BCS curve in Figs. 5 and 6. Although there is no doubt in some distribution in the amplitudes of the gaps, the similarity of C'_{es} with that of MgB_2 suggests that it is relatively narrow. The breadth of the transition is no doubt partly a consequence of inhomogeneity in the sample, but there is also reason to think that fluctuations are important (see Sec. IV C). These two effects cannot be reliably separated, but two possibilities are represented in the inset of Fig. 6.

For sample 3 there is no evidence of a T^2 dependence of C'_{es} that would indicate the presence of line nodes. However, in the context of results on the cuprates, Scalapino[37] showed that in the presence of strong pair breaking the T^2 term can be obscured by the $\gamma_r T$ term. The presence of line nodes is

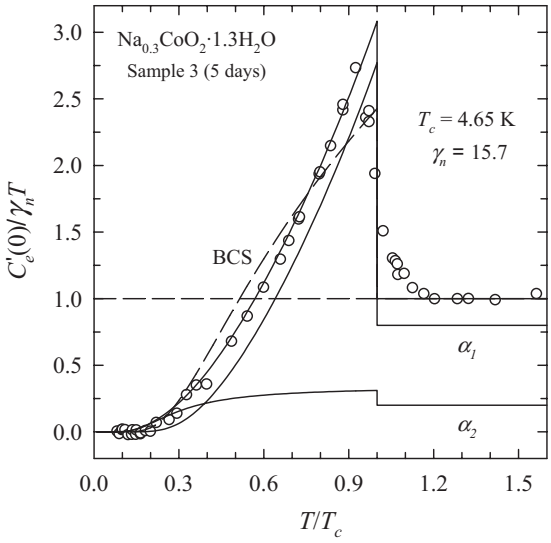

FIG. 7. The zero-field electron specific heat of sample 3, normalized to 1 mol of superconducting condensate (see Sec. III B), compared with BCS theory and a two-gap fit, without nodes. For $T \leq T_c$, $C_e'(0) = C_{es}'$.

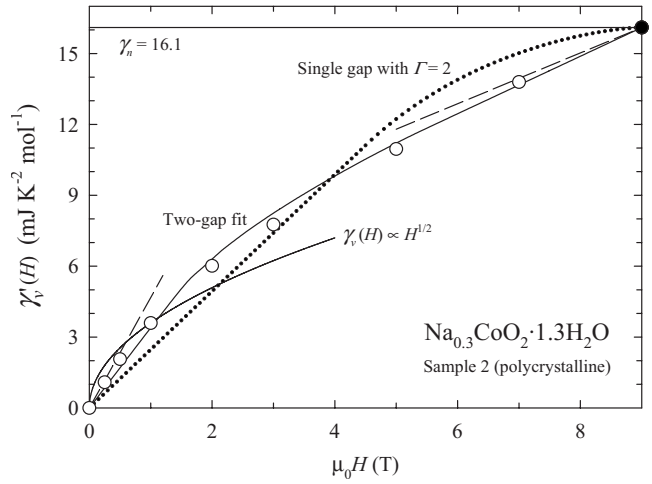

FIG. 8. The coefficient of the T-proportional term in the superconducting- and vortex-state specific heat (open circles) obtained as described in Sec. VI and the normal-state value (solid circle) obtained as described in Sec. IV A. The values plotted are normalized to 1 mol of superconducting condensate (see Sec. III B). The dashed lines represent two-gap fits to the limiting slopes that are described in the text. The solid curves represent an $H^{1/2}$ dependence and a two-band fit, which are described in the text. The dotted curve is calculated for a single band with an anisotropic H_{c2} and $\Gamma = 2$, as described in the text.

therefore not ruled out. As shown in Fig. 7, the deviations from BCS theory are not as conspicuous as for sample 2. However, they still suggest two gaps. Although the positive deviations at low temperature associated with the small gap are not evident in Fig. 7, the high values of C_{es}' and positive curvature of C_{es}'/T near T_c are signatures of strong coupling, i.e., $\alpha > 1.764$, and evidence of the presence of the large gap. The best single-gap fit, which approximates the data near T_c, underestimates C_{es}' at low temperatures where the small-gap contribution is important. The best fit—a two-gap α-model fit without nodes—with $\alpha_1 = 2.30$, $\alpha_2 = 1.10$, $\gamma_{1s}/\gamma_n, = 0.24$, and $\gamma_{2s}/\gamma_n = 0.06$, is shown in Fig. 7. The substantial reduction in the contribution of the small-gap band to the superconducting condensate relative to that for sample 2 accounts for the qualitative difference in C_{es}' for the two samples. The data are also well represented by a more fundamental two-band fit by Bussmann-Holder[38] with s-wave pairing in both bands and the interaction potentials and the temperature dependence of the gaps determined self-consistently.

For a conventional type-II superconductor, normal-state-like excitations in the vortex cores give a T-proportional term in the vortex-state specific heat, and its coefficient, $\gamma_v(H)$, is expected to be linear in H, reflecting the linear increase in number of vortices.[39,40] However, as shown in the inset of Fig. 4 and in Fig. 8, where $\gamma_v(H)$ is represented by $\gamma_v'(H)$, there is substantial curvature. Line nodes in the gap give an $H^{1/2}T$ dependence for C_{es} for $(H_{c2}/H)^{1/2}T/T_c < 1$.[41] The data do not extend into that region of H and T, and the finite slope of $\gamma_v'(H)$ at $H=0$ is inconsistent with an $H^{1/2}$ dependence. However, an $H^{1/2}$ dependence in that region has been reported,[13,14] and a curve of that form has been included in Fig. 8 for comparison. The curvature of $\gamma_v'(H)$ is qualitatively similar to that of the power-law dependence, for a wide range of H, derived by Nakai *et al.*[42] for a two-gap superconductor and compared with experimental results for MgB_2, H^α (with $\alpha = 0.3$ for MgB_2). However, a simple power law is not consistent with the experimental results over the whole range of H. For MgB_2 Bouquet *et al.*[43] showed that $\gamma_v(H)$ is well approximated in the low-H and near-H_{c2} limits as the sum of contributions from the two bands, each of which is linear in H to an effective H_{c2} for that band, H_{c2}^i, and saturates at that point. The $H=0$ and $H=H_{c2}$ limiting slopes, represented by the dashed lines in Fig. 8, provide the basis for an interpretation of this type; in principle, the slopes of the linear-in-H contributions are γ_{is}/H_{c2}^i. Since H_{c2} varies as $[\Delta(0)/v_F]^2$, where v_F is the Fermi velocity, it is reasonable to identify the large-gap band with the larger of the two H_{c2}^i and the numerical value of 9 T, giving $\mu_0 H_{c2}^1 = 9$ T. The γ_{is} were determined in the two-gap analysis of C_{es}, leaving *one* of the four parameters to be determined, but there are *two* additional conditions that must be satisfied: the limiting slope at $\mu_0 H = 9$ T is γ_{1s}/H_{c2}^1 and the limiting slope at $H = 0$ is that of the sum of the two contributions, $\gamma_{1s}/H_{c2}^1 + \gamma_{2s}/H_{c2}^2$. Consequently, different fits to the limiting slopes are possible, depending on which two of the three known parameters are taken to be fixed. Taking the values of γ_{is} from the two-gap fit gives $\mu_0 H_{c2}^2 = 2.0$ T and $\mu_0 H_{c2}^1 = 8.1$ T (instead of 9 T); taking $\mu_0 H_{c2}^1 = 9$ T and requiring only that the *sum* of the values of γ_{1s} and γ_{2s} be that obtained in the two-gap fit gives $\mu_0 H_{c2}^2 = 1.8$ T, $\gamma_{1s}/\gamma_n = 0.36$ (instead of 0.33), and $\gamma_{2s}/\gamma_n = 0.24$ (instead of 0.27). Given the uncertainties in the various parameters and in the experimental values of $\gamma_v(H)$, these approximate "fits" to $\gamma_v(H)$ are reasonably consistent with the parameters derived from the two-gap fits to C_{es}. Furthermore, taking $\alpha_1 = 2.20$ and $\alpha_2 = 1.00$ as representative measures of $\Delta_1(0)$ and $\Delta_2(0)$ obtained in the fits to C_{es} (see Sec. VII), $[\Delta_1(0)/\Delta_2(0)]^2 = 4.8$, accounting satisfactorily for the ratios H_{c2}^1/H_{c2}^2, 4.1 or 5.0, respectively.

However, it is clear that projections of the limiting slopes would not represent the experimental data at intermediate values of H. For a strongly 2D, but axially symmetric, material such as $Na_{0.3}CoO_2 \cdot 1.3H_2O$ anisotropy of H_{c2}, characterized by $\Gamma = H_{c2\parallel ab}/H_{c2\perp ab}$, where $H_{c2\parallel ab}$ and $H_{c2\perp ab}$ are H_{c2} for H parallel and perpendicular to the ab plane, can also be expected to produce curvature in $\gamma_v(H)$. Several measurements of electrical resistivity[10,22] suggest $\Gamma \sim 4-6$, but the magnitudes of the deviations from linearity are more consistent with $\Gamma = 2$. The dotted curve in Fig. 8 represents $\gamma_v(H)$ as calculated for a single-band superconductor with $\Gamma = 2$ using the effective-mass approximation[44] for the anisotropy of H_{c2}. The deviations from the experimental results are conspicuous. Higher values of Γ would shift the calculated curve to higher values of $\gamma_v(H)$ for all H, showing that the experimental results cannot be understood in terms of a single band with an anisotropic H_{c2} and any value of Γ. Comparison of the nearly linear behavior of $\gamma_v(H)$ for $\mu_0 H > 5$ T with the calculations for anisotropic H_{c2} also shows that H_{c2} for the large-gap band must be nearly isotropic. Even with this constraint, however, a number of two-band anisotropic-H_{c2} fits to $\gamma_v(H)$ are possible if the parameters are allowed to some latitude. One example, for which $\gamma_{1s}/\gamma_n = 0.39$, $\gamma_{2s}/\gamma_n = 0.21$, $\mu_0 H_{c2}^1 = 9$ T, $\mu_0 H_{c2}^2 = 6.5$ T, $\Gamma = 1$ for the large-gap band, and $\Gamma = 4$ for the small-gap band, is represented by a solid curve in Fig. 8. The general shape of $\gamma_v(H)$ is consistent with contributions from two bands, but it is not possible to obtain a good fit with the parameters obtained from the two-gap analysis of C_{es}. In evaluating the validity of any of these interpretations of $\gamma_v(H)$ the uncertainty in the experimental values, which was noted in Sec. IV C, should be kept in mind.

VII. PHENOMENOLIGICAL INTERPRETATION OF THE SPECIFIC HEAT AND ITS DEPENDENCE ON SAMPLE AGE

The pair breaking, as measured by the residual density of states, increases with sample age: for sample 2 (3 days) $\gamma_r/\gamma_n = 0.40$, for sample 3 (5 days) $\gamma_r/\gamma_n = 0.70$, for sample 1 (40 days), there is no superconductivity, and for the purpose of comparison with the superconducting samples the pair breaking is complete and γ_r/γ_n is in effect 1.00 (even though the normal-state DOS is reduced by 24% by the 7 K transition). The difference in C'_{es} between samples 2 and 3 is produced by the pair breaking, which occurs preferentially in the band in which the pairing is weaker, the small-gap band, and shifts the relative contributions of the bands to the superconducting condensate. For sample 1 the pair breaking is even stronger; the electron pairing of the superconducting state has been weakened to the point that it has given way to a competing order, CDW order. On the basis of sample age the differences in the specific heat of samples 2, 3, and 1 can be related to the time dependences of other properties that have been recognized recently. Several studies[18,19] have shown that samples that are not superconducting (or at least have T_c below the minimum that could be detected) become superconducting, T_c passes through a maximum, ~ 4.5 K, and then decreases. The time scale for these changes is on the order of days but, not surprisingly, it appears to depend on storage conditions. The work of Barnes *et al.*[19] is particularly relevant to the specific heat. They have shown that the changes in T_c are accompanied by changes in the lattice parameters that are associated with changes in the concentration (δ) of O vacancies. The concentration of O vacancies increases with time, starting before superconductivity appears (in these measurements at ~ 2 K) and continuing after it has disappeared. They note that "samples that show no superconductivity may simply have gone through their *life cycle* before being studied" and emphasize the importance of consideration of "time-dependent phenomena" in interpreting experimental data. The similarity in the time scales for changes in the specific heat, particularly the increase in the residual DOS, and changes in the concentration of O vacancies, together with the fact that the O vacancies occur in the conducting planes, suggests the identification of the O vacancies as the pair-breaking centers. (It seems unlikely that disorder in the Na or H_2O layers would produce the pair breaking, and the O vacancies are the only plausible candidate.) Identification of the O vacancies with the pair-breaking centers accounts for the fact that sample 3, with a higher value of δ, has a higher residual DOS than sample 2, while sample 1, with an even higher δ, was not superconducting.

The change in O stoichiometry with sample age implies a change in carrier concentration that might be expected to affect the normal-state DOS and other properties that depend on details of the band structure. However, such effects are not large enough to be identified in the specific-heat results. The coefficient of the normal-state electron specific heat (16.1, 15.7, and 16.4 mJ K^{-2} mol^{-1} for samples measured after 3, 5, and 40 days, respectively) does not demonstrate a systematic dependence on sample age. Furthermore, the values were obtained by slightly different analyses (see Sec. VIII). Different values of the gap parameters were obtained for samples 2 and 3 (for sample 2, $\alpha_1 = 2.15$ and $\alpha_2 = 1.00$ by one analysis and $\alpha_1 = 2.20$ and $\alpha_2 = 0.70$ by another; for sample 3, $\alpha_1 = 2.30$ and $\alpha_2 = 1.10$) but the differences between those for sample 2 and those for sample 3 are comparable to the differences between values obtained for sample 2 by different analyses. Approximations inherent in the derivation of these quantities, in the α model itself, and in the separation of C'_{es} into two components, as well as the small contribution of the small-gap band to C'_{es} in sample 3, all contribute to uncertainty in the values obtained. We conclude that the differences in the values of α_1 and α_2 obtained for samples 2 and 3 are probably not significant, and in the following we take $\alpha_1 = 2.20$ and $\alpha_2 = 1.00$ as representative measures of the gap parameters.

With the assumption that secondary effects of the pair-breaking centers on band structure can be neglected, the evolution of the specific heat of the superconducting samples with increasing sample age can be understood on the basis of a simple, but plausible, two-band model. The model incorporates three assumptions: (1) the total contribution of each band to the DOS is the same for all samples; (2) for a particular sample the contributions of the bands to the total DOS are divided between the residual DOS and the superconducting condensate in proportions determined by the concentration of pair-breaking centers; and (3) the relative contribu-

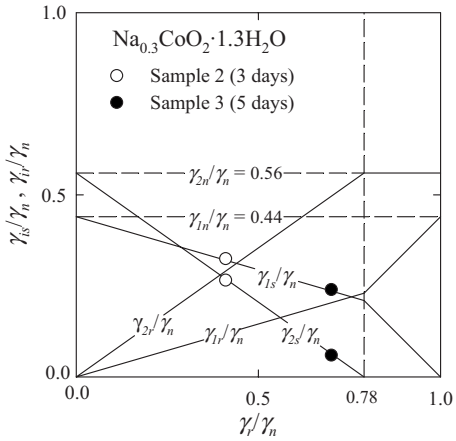

FIG. 9. The contributions of the two electron bands to the superconducting condensate and to the residual DOS as functions of the total pair breaking. All quantities are shown as fractions of γ_n: γ_{is}/γ_n and γ_{ir}/γ_n for the contributions to the superconducting condensate and to the residual DOS, respectively, and γ_r/γ_n for the total pair breaking. The experimental points for γ_{is}/γ_n for samples 2 and 3 are from two-gap fits to C_{es}. The straight-line constructions for both γ_{is}/γ_n and γ_{ir}/γ_n are based on the assumption that each band makes the same fractional contribution to the pair breaking for all samples, and they are determined by the experimental points for samples 2 and 3. For $\gamma_r/\gamma_n \geq \gamma_r^*/\gamma_n = 0.78$, the small-gap band makes no contribution to the superconducting condensate, and the additional pair breaking is entirely in the large-gap band; $\gamma_{2s}=0$, $\gamma_{2r}=\gamma_{2n}$, and γ_{1r} increases linearly to γ_{1n}.

tions of the two bands to the residual DOS are determined by the relative strengths of the pairing interactions in the bands and are in the same proportion for all samples. In quantitative terms (with all quantities measured by the equivalent contributions to γ_n) (1) the contribution of a band to the total DOS is γ_{in}, where $\gamma_{1n}+\gamma_{2n}=\gamma_n$, (2) for different samples, the γ_{in} are divided between contributions to the residual DOS and the superconducting condensate, γ_{ir} and γ_{is}, respectively, which are different for different samples, but $\gamma_{ir}+\gamma_{is}=\gamma_{in}$ for all samples, and (3) the contribution of a band to the residual DOS, γ_{ir}, is the same fraction of γ_r for all samples; $\gamma_{ir}=x_i\gamma_r$, where the x_i are constants and $x_1+x_2=1$. It follows that the γ_{is} are also linear in γ_r: $\gamma_{is}=\gamma_{in}-\gamma_{ir}=\gamma_{in}-x_i\gamma_r$. The model is represented graphically in Fig. 9, where γ_{ir} and γ_{is} are represented as fractions of γ_n and shown as functions of the total pair breaking, represented by γ_r/γ_n. In quantitative terms, it is completely defined by the values of x_1 and x_2, 0.28 and 0.72, respectively, derived from the values of γ_{is} for samples 2 and 3 that were obtained in the two-gap fits to C_{es}. The ratio of the pair breaking in the small- and large-gap bands ($x_2/x_1=0.72/0.28=2.6$) is comparable to the inverse of the ratio of the pairing strengths as measured by the gap parameters ($\alpha_1/\alpha_2=2.20/1.00=2.2$), which supports the validity of the model. The stronger pair breaking in the small-gap band leads to the disappearance of the contribution of that band to the superconducting condensate at $\gamma_r^*/\gamma_n=0.78$, where $\gamma_{2s}=0$. For $\gamma_r/\gamma_n>0.78$ additional pair breaking occurs only in the large-gap band, γ_{1r} increases linearly to γ_{1n}, $\gamma_{2s}=0$, and $\gamma_{2r}=\gamma_{2n}$. This provides an estimate of the contributions of both bands to the normal-state DOS. At $\gamma_r/\gamma_n=0.78$, $\gamma_{2n}=\gamma_{2r}=x_2\gamma_r=0.72(0.78\gamma_n)=0.56\gamma_n$ and $\gamma_{1n}=\gamma_n-\gamma_{2n}=0.44\gamma_n$.

For $Na_xCoO_2 \cdot 1.3H_2O$, as for the cuprates, T_c exhibits a dome-shaped dependence on carrier concentration.[20] Changing the Na content produces a symmetric dome,[20] similar to that of the cuprates. Changes in the concentration of O vacancies produce a dome of similar width, but asymmetric in form, with T_c decreasing precipitously on the high-O-vacancy (low-Co oxidation state) side[19] (see Fig. 9 of Ref. 19). Barnes *et al.*[19] noted this difference with the cuprates and suggested, as one possibility, that after T_c reaches its maximum "some other instability destroys superconductivity." Apparently, the pair-breaking action of the O vacancies produces that "instability." The O vacancies have two competing roles in the superconductivity: at low concentrations, an increase adjusts the carrier concentration to produce an increase in T_c; at higher concentrations a further increase destroys the superconductivity by pair-breaking. Limits to the occurrence of superconductivity and the values of T_c are not well defined in relation to the γ_r/γ_n axis of Fig. 9. Taking T_c for samples 2 and 3 at face value, these samples either straddle or are on the low-O-vacancy side of the maximum T_c, but in any case they are certainly close to the maximum. Barnes *et al.*[19] could not detect T_c below ~ 2 K, and it is not clear whether superconductivity extends to $\gamma_r/\gamma_n=0$, with low T_c, or whether it disappears. The limit to the occurrence of superconductivity on the high γ_r/γ_n side is also not clear. The straight-line constructions in Fig. 9 are shown for $0 \leq \gamma_r/\gamma_n \leq 1$, but neither the assumption on which they were based nor the conclusions drawn from them depends on the occurrence of superconductivity over the whole of that range. The association of the sample-to-sample differences in C_{es} with pair breaking by the O vacancies has implications for possible values of γ_r. High values of T_c are associated with substantial concentrations of O vacancies,[19] which suggests that any sample with a high T_c will also have a substantial γ_r. Unlike the cuprates and heavy-fermion superconductors, improvements in "sample quality" may not lead to samples with small γ_r.

VIII. COMPARISON WITH OTHER SPECIFIC-HEAT MEASUREMENTS: EVIDENCE FOR THE "INTRINSIC" NATURE OF THE SPECIFIC-HEAT RESULTS—NORMAL-STATE DENSITY OF STATES

The claim that the measured properties of our samples are intrinsic in the sense that they are the properties of well-defined (albeit unstable) materials and not the result of unrecognized random defects or poor sample quality is supported to some degree by the absence of the evidence of poor sample quality that was seen in early measurements on the cuprates, upturns in $C(0)/T$ at low T, and other evidence of paramagnetic centers that were associated with the sample dependence of the specific heat, particularly the sample-dependent residual DOS. More compelling evidence is provided by comparisons with other samples of $Na_{0.3}CoO_2 \cdot 1.3H_2O$ that show the same combinations of different features in the specific heat—the residual DOS, details of the temperature dependence of C'_{es}, the occurrence of su-

perconductivity, and the occurrence of the 7 K anomaly. The specific heats of samples 2 and 3 and the differences between them are closely matched by those of another pair of samples, samples A and B, studied by Yang *et al.* (Refs. 13 and 12, respectively). C'_{es} and the residual DOS are similar for samples 2 and A; they are also similar for samples 3 and B but different from those for samples 2 and A. For samples 2 and A, $C_e(0)/T$ is approximately linear in T for $1<T<3$ K, suggesting the presence of nodes in the energy gap; for samples 3 and B, it shows substantial positive curvature, which is more consistent with the absence of nodes. The similarity of samples 2 and A and their differences with samples 3 and B can be characterized more quantitatively by comparisons of parameters derived from C_{es} and C'_{es}. For sample A, $\gamma_r/\gamma_n=0.53$, $\Delta C'_{es}(T_c)/\gamma_n T_c=1.45$, and $T_c=4.5$ K (cf. 0.40, 1.35, and 4.52 K for sample 2). For sample B, $\gamma_r/\gamma_n=0.73$, $\Delta C'_{es}(T_c)/\gamma_n T_c=1.96$, and $T_c=4.7$ K (cf. 0.70, 2.08, and 4.65 K for sample 3). None of these four samples showed evidence of the 7 K transition. The comparisons with other samples can be extended to include sample 1; specific-heat measurements on two other samples[6,9] showed the anomaly at 7 K but none near 4.5 K. In both cases, a superconducting transition had been observed near 4.5 K, by susceptibility[6] or transport[9] measurements, but the superconductivity was not present when the specific heat was measured. Thus, the features in the specific heat of all three of our samples and the correlations among them are matched by those of other samples.

The major features of the vortex-state specific heat of sample 2 are also similar to those of sample A.[13] Except at the lowest temperatures, $C_e(H)$ is qualitatively similar for both samples, and the temperature of the onset of the transition to the vortex state is independent of the applied field for both samples. The latter effect has also been noted in measurements on sample B.[12] However, neither the $H^{1/2}$ dependence of $\gamma_v(H)$, which is expected at low T for line nodes,[41] nor the sharp increase at low H reported in Ref. 13 is apparent in our data. Jin *et al.*[14] also reported an $H^{1/2}$ dependence of $\gamma_v(H)$. It should be noted that none of these measurements extend into the range of H and T in which the $H^{1/2}T$ term is expected, and the reported $H^{1/2}$ dependences do not fully conform to the theoretical prediction in that they are found by extrapolation from regions where $C_e(H)$ includes a T^2 term.

Jin *et al.*[14] reported a precipitous drop in $C_e(H)/T$ at $T_x \sim 0.8$ K, the "anomaly at T_x." This feature is not seen in other data, but it has been cited by Mochizuki *et al.*[45] as evidence of a role of the e'_g hole pockets in the superconductivity of *that* sample. Mochizuki *et al.*[45] noted the similarity of our sample 2, sample A of Yang *et al.*,[12,13] and the sample of Jin *et al.*[14] for $T>\sim 1$ K. However, they apparently assumed that there would be a sharp drop in C_{es} for sample 2 at lower T, similar to, but steeper than that associated with the anomaly at T_x, and compared a *theoretical extrapolation* of the sample 2 data with the *experimental* results reported by Jin *et al.*[14] They concluded that the Fermi surface and the OP were different for the two samples. They attributed the differences to a difference in Na content and its effects on interlayer spacing and the Fermi surface. (A more detailed comparison of their model with the experimental results is included in Sec. IX.) The *measurements* on sample 2 and particularly those on sample A extend well into the region of negative curvature of C/T vs T that is associated with the anomaly at T_x but show no hint of deviation from linearity. The similarity in specific heat and the similarity in T_c of all three samples suggest that significant differences in Na content are unlikely. These comparisons raise the question of whether the anomaly at T_x might be a consequence of experimental error and that possibility is also suggested by the specific heat in magnetic fields. In the vicinity of T_x, the specific heat drops precipitously for *all* H, including $\mu_0 H=14$ T, for which the anomaly at T_c is completely suppressed and the sample is in the normal state, but the specific heat is *lower* than in zero field. Other features of the specific-heat results of Jin *et al.*[14] suggest the presence of magnetic impurities, which could give a substantial magnetic contribution to the specific heat in the region of the anomaly at T_x, and this is also the T region in which there is a substantial hyperfine contribution. Since the measurements were made by the relaxation method, these large contributions to the specific heat, in combination with the low thermal conductivity that is characteristic of this T region, could lead to long-time constants for internal thermal equilibrium and incorrect results. The measurements by Jin *et al.*[14] also show another unusual feature that is not seen in either sample 2 or sample A, an H-induced approximately T-independent increase in C/T in the normal state, i.e., an apparent increase in γ_n [see Fig. 3(a) of Ref. 14].

The coefficient of the normal-state electron specific heat, γ_n, is of special interest as a measure of the normal-state DOS, but a wide range of experimental values, 10.8–16.6 mJ K^{-2} mol^{-1}, has been reported. They were obtained by several different methods of analysis of the data, the most common of which would give values that are too low. The value 16.1 mJ K^{-2} mol^{-1} for sample 2 was obtained using normal-state data that extended to ~ 1 K. (The presence of excess water could lead to error in the number of moles of sample, and, as noted below, it can lead to error in values of γ_n obtained by extrapolation of high-T C/T data to 0 K. For sample 2, the number of moles of sample was obtained by a quantitative analysis for Co.) Apparently all other values have been obtained using less direct methods. For sample 3, γ_n was obtained by fitting $C(0)$ in the range of 6–12 K with $C(0)=\gamma_n T+C_{lat}$ and the constraint that the fit give the correct entropy at 6.5 K, which was determined by zero-field data to 0.3 K. A good fit required three terms in C_{lat} and gave $\gamma_n=15.7$ mJ K^{-2} mol^{-1}. The same procedure, but using a higher-T fitting interval, which was required by the 7 K anomaly, gave 16.4 mJ K^{-2} mol^{-1} for sample 1. A similar procedure, but using only two terms in C_{lat}, has given lower values, 14.9 and 13.9 mJ K^{-2} mol^{-1} (Refs. 12 and 13, respectively), and two values that are among the lowest reported, 10.8 and 12.5 mJ K^{-2} mol^{-1}, were obtained with two terms in C_{lat} but without data below ~ 2 K to determine the entropy.[11] All other values[5–10,13] were obtained by a linear extrapolation of a plot of C/T vs T^2 from above ~ 6 to 0 K. The validity of these extrapolations would require T^3 behavior of C_{lat} to implausibly high temperatures, but C/T is surprisingly linear in T^2, at least from 6 to 12 K, which seemed to justify the extrapolations. The linearity for $6\leq T\leq 12$ K is

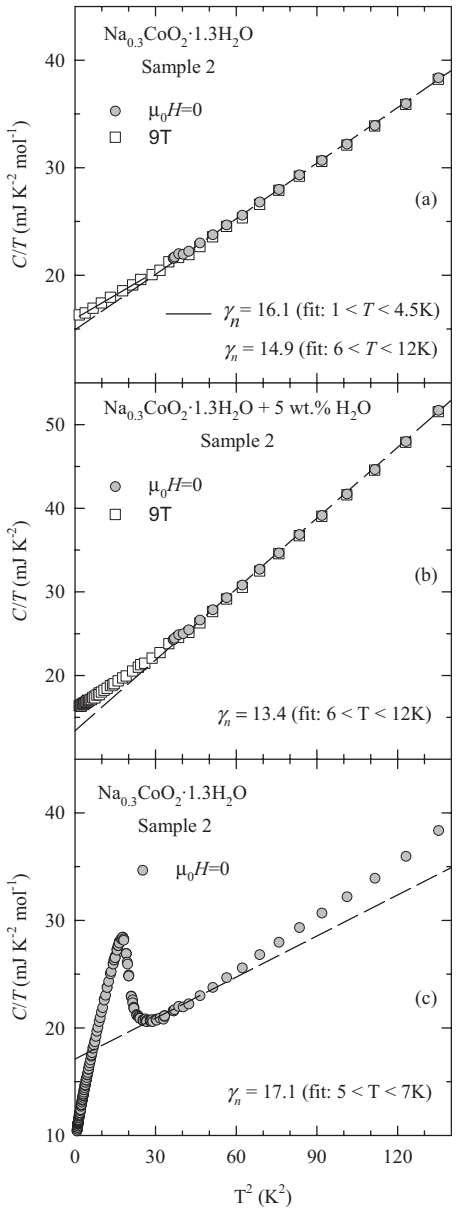

FIG. 10. Specific heat of sample 2 plotted as C/T vs T^2 to illustrate the origin of possible errors in values of γ_n obtained by straight-line extrapolations in such plots.

illustrated by normal-state data for sample 2 in Fig. 10(a), which, however, also shows curvature and a relatively sharp change in slope in the vicinity of 6 K that would cause the extrapolation to give a low value of γ_n. As demonstrated in Fig. 10(a), a linear extrapolation from the 1–4.5 K interval gives 16.1 mJ K^{-2} mol^{-1}, the same value obtained by the four-parameter fit to 12 K, but a linear extrapolation from the 6–12 K interval gives 14.9 mJ K^{-2} mol^{-1}. The curvature also emphasizes the importance of including enough terms in C_{lat} in any treatment of the data. Many of the values of C/T in the 6–12 K interval are higher than those for sample 2 in a few cases by almost a factor 2. The presence of excess water is a possible explanation, as suggested in Fig. 10(b), which shows the same sample 2 data increased by the addition of the heat capacity of 5 wt. % water, to give values of C/T near the middle of the range of those reported. Between 6 and 12 K, C/T is still remarkably linear in T^2, but the curvature in the vicinity of 6 K is more pronounced, and the extrapolations from 6 to 12 K interval give a still lower value, 13.4 mJ K^{-2} mol^{-1}. Figure 10(c) shows the zero-field sample 2 data and demonstrates how an extrapolation from temperatures that are too close to T_c could give a high value of γ_n, 17.1 mJ K^{-2} mol^{-1}. Since the possible errors associated with other methods of obtaining γ_n can easily account for the discrepancies with the value obtained directly from low-T normal-state data, there is no reason to think that there might be real differences in γ_n for different samples, and we suggest 16.1 mJ K^{-2} mol^{-1} as the most reliable value.

IX. COMPARISON WITH BAND-STRUCTURE RESULTS

Band-structure calculations give $N(E_F)$, the band-structure DOS at the Fermi level, and its equivalent, the "band structure γ," γ_{bs}, which is $2.36N(E_F)$, in mJ K^{-2} mol^{-1} if $N(E_F)$ is in states eV^{-1} with the spin degeneracy included. The γ_n determined experimentally by specific-heat measurements includes enhancements of the DOS by both electron-phonon and electron-electron interactions. With the exception of heavy-fermion compounds, the correction to the calculated DOS for electron-electron interactions is generally thought to be small and is frequently neglected. It does not seem to have been considered in connection with $Na_{0.3}CoO_2 \cdot 1.3H_2O$, and we neglect it in the following. The electron-phonon enhancement is represented by a factor $1+\lambda$, where λ is a measure of the strength of the interaction, and $\gamma_n = (1+\lambda)\gamma_{bs}$. A comparison of γ_{bs} and γ_n can confirm the validity of the calculations and/or provide an estimate of the phonon enhancement. For $Na_{0.3}CoO_2 \cdot 1.3H_2O$, however, all such comparisons are compromised by uncertainties in the theoretical predictions that derive from the difficulty in treating exchange and correlation effects of the d electrons. Although most band-structure calculations have been made on simplified models for the unhydrated compounds in which there is one Co per unit cell and the positions and effects of the H_2O and Na are approximated in one way or another, this seems to be a less serious problem. The contrast with MgB_2 is striking. For s/p-electron MgB_2, a number of independent calculations give similar results, and the more detailed calculations give a complete description of the two-band nature of the Fermi surface and the superconductivity; for the d-electron cobaltate superconductor the nature of the Fermi surface—two bands or one—and the value of $N(E_F)$ depend on the treatment of exchange and correlation effects, with the latter varying by a factor that approaches 10, and there are no calculations for the superconducting-state parameters comparable to those for MgB_2.

The band-structure calculations for Na_xCoO_2 include calculations within the local-density approximation (LDA) and calculations within the spin-polarized local-density approximation (LSDA), which allows for the possibility of the spin polarization that is suggested by observed tendencies to magnetic order and the narrow bandwidths, and extensions of both that take into account strong on-site Coulomb interac-

tions represented by the Hubbard U, the LDA+U, and LSDA+U methods. The first calculation, which predated the discovery of superconductivity in the hydrated compound, was done by Singh[46] for $NaCo_2O_4$ (i.e., for $x=0.5$ in Na_xCoO_2, but two Co in the unit cell). The crystal field of the O octahedra splits the Co 3d states into triplet t_{2g} and higher-lying doublet e_g manifolds and a rhombohedral crystal field produced by the distortion of the O octahedra splits the t_{2g} states into four e_g bands, which were denoted e_g' to distinguish them from the higher-lying e_g manifold, and two a_{1g} bands. The a_{1g} and e_g' bands determine the Fermi surface, producing, respectively, a large cylindrical hole section at the zone center and six small surrounding hole pockets. The total DOS at the Fermi energy was $N(E_F)=4.4$ eV^{-1} (per Co) within LDA, and an LSDA calculation for ferromagnetic ordering gave a slightly lower energy and $N(E_F)=4.1$ eV^{-1}. In a tight-binding calculation for $x=0.33$ Johannes *et al.*[47] found $N(E_F)=8.9$ eV^{-1} with 2/3 of the total DOS contributed by the e_g' pockets. Johannes and Singh[48] made calculations for $Na_{0.33}CoO_2\cdot 1.33H_2O$ that explicitly included the H_2O and Na ions, in a unit cell that included 6 f.u., and compared the results with those for the same unit cell but without the H_2O and with the c-axis dimension of the unhydrated material. They showed that the major effect of the H_2O was purely structural, the changes in interplanar coupling and 2D character associated with the increase in the c dimension, but they note that "the effect of water's particular role in the superconductivity is still very open." The main features of Singh's original results[46] have been reproduced in more recent calculations and extended to other doping levels and to the inclusion of the on-site U. Zhang *et al.*[49] compared the results of LDA, LSDA, and LSDA+U calculations for $x=0.3$, 0.5, and 0.7. They found that relative to the Fermi energy the e_g' band was raised with decreasing x, increasing the size of the e_g' pockets, lowered in LSDA relative to LDA, and strongly lowered in LSDA+U. The hole pockets existed in LDA only for $x=0.3$ and 0.5; in LSDA, only for $x=0.5$; and in LSDA+U, not at all. Band-structure calculations relevant to the existence of the e_g' pockets have also been reported in a number of other papers.[50–57] LDA+U and LSDA+U calculations generally show that the e_g' pockets are suppressed by the on-site Coulomb interactions. That conclusion is both supported[53] and contradicted[54,57] by other treatments of the interactions. Other calculated values of $N(E_F)$ for $x\sim 0.3$ (with the type of calculation included in the parentheses) include 1.0 eV^{-1} (LSDA+U, Ref. 50), 3.6 eV^{-1} (LDA, Ref. 51), 4.58 eV^{-1} (tight-binding-dynamical mean-field theory, Ref. 54), 6.2 (LDA, Ref. 56), and 1.6 eV^{-1} (LDA+U, Ref. 56). In the wide range of values of $N(E_F)$ notwithstanding, there is a clear separation between those reported for a Fermi surface that includes both the a_{1g} and e_g' surfaces and those reported for the a_{1g} surface alone, whether the e_g' surface exists or not. The former fall in the range 4–9 eV^{-1}; the latter in the range 1–3 eV^{-1}. The distributions of values in the two groups suggest 5 and 1.5 eV^{-1} as reasonably representative values, which correspond to $\gamma_{bs}=12$ and 3.5 mJ K^{-2} mol^{-1}, respectively. Comparisons with $\gamma_n=16.1$ mJ K^{-2} mol^{-1} give a strong but plausible phonon enhancement for the former but a seemingly impossible value for the latter. These comparisons suggest that the theoretical results cannot account for the experimentally observed DOS without the e_g' pockets.

Mochizuki *et al.*[45] derived the energy-gap structure and specific heat for two different Fermi surfaces that might exist for $Na_{0.3}CoO_2\cdot 1.3H_2O$ samples with different Na and H_2O contents. One of them, FS1, consists of two concentric a_{1g} cylinders and gives spin-singlet pairing and an extended s-wave OP; the other, FS2, consists of a single a_{1g} cylinder and the six e_g' pockets and gives spin-triplet pairing with a p-wave OP. Mochizuki *et al.*[45] suggested that our sample 2 is an example of FS1 and the sample studied by Jin *et al.*[14] is an example of FS2. They claim to "show that the two different $C(T)$ data reported by Oeschler *et al.*[16] and Jin *et al.*[14] are reproduced for each pairing state." For both FS1 and FS2 the calculated C_{es} is obtained as the sum of contributions of the two bands, one of which is very similar to the contribution of the large-gap band and the other to that of the small-gap band, obtained in the empirical two-gap fit to the sample 2 data in Sec. VI [see Figs. 3(a), 3(b), and 6 of Ref. 45]. In the theoretical result, the large-gap surface is an a_{1g} cylinder for both FS1 and FS2; the small-gap surface is the other a_{1g} cylinder for FS1 and the e_g' pockets for FS2. For $T>\sim 0.9$ K the large-gap contributions are essentially the same for both FS1 and FS2 and account for most of the T-dependent part of C_{es}/T. In that T interval C_{es}/T, which is essentially the same for both samples, is well accounted for by the theoretical calculations but does not test the differences predicted for FS1 and FS2. It is only for $T<\sim 0.9$ K, where the large-gap contributions are negligible, that experimental data could test the theoretical predictions for FS1 and FS2. For the FS2 calculation C_{es}/T goes to zero as T, corresponding to line nodes seen in the calculated energy gap. The experimental data of Jin *et al.*[14] decrease somewhat more rapidly, but, more importantly, there is reason to question their validity (see Sec. VIII). For the FS1 calculation C_{es}/T goes to zero more steeply, presumably exponentially, corresponding to the s-wave OP. In effect, the $\gamma_r T$ term and the small-gap contribution of our empirical analysis are lumped together and replaced with a larger small-gap contribution with a smaller gap. Since there are no experimental data, the only basis for comparison of the experimental and theoretical results is the entropy at T_c. The theoretical result gives a discrepancy of 5%, while the consistency of the extrapolations of the experimental data for different fields is better than 1%. Thus, while the calculations of Mochizuki *et al.*[45] provide an interesting confirmation of the validity of the two-gap two-band interpretation of C_{es}, the experimental data do not support the conjecture of different Fermi surfaces for sample 2 and the sample of Jin *et al.*[14]

Angle-resolved photoelectron spectroscopy (ARPES) measurements for a wide range of x show the a_{1g} contribution to the Fermi surface, in agreement with theoretical predictions, but have consistently failed to show the presence of the e_g' pockets.[58–63] With one exception, the measurements of Shimojima *et al.*[63] on a hydrated superconducting sample, the measurements were made on unhydrated Na_xCoO_2. An interesting result of the measurements on the superconducting sample is that, while the e_g' band does not cross the Fermi energy, it is only 30 meV below, much less than the 200 meV in the corresponding unhydrated material.[63] In contrast to the

ARPES measurements, the Shubnikov–de Haas effect in Na_xCoO_2 for $x=0.5$ and 0.3 (Refs. 64 and 65, respectively) shows clear evidence of small-cross-section elements of the Fermi surface. As noted in Ref. 65, the Shubnikov–de Haas frequencies for $x=0.3$ are in good agreement with the cross sections of the e_g' pockets obtained in an LDA calculation[46] for $x=0.5$. Particularly in view of the possible competing effects of decreasing x and the Coulomb correlations on the e_g' pockets,[49] that agreement could be taken as evidence that the Shubnikov–de Haas frequencies are associated with the e_g' pockets, but the authors ruled out that interpretation on the grounds that the experimental γ_n did not allow for the existence of both the a_{1g} and e_g' surfaces. That conclusion, however, was based on a value for γ_n, 12 mJ K^{-2} mol^{-1}, which is probably too low (see Sec. VIII) and a relatively high estimate of the contribution of the a_{1g} surface. With $\gamma_n = 16.1$ mJ K^{-2} mol^{-1} (see Sec. VIII) and reasonable allowances for uncertainties in the calculated values of $N(E_F)$ and in the experimental results, the e_g' pockets are a more plausible origin of the observed Shubnikov–de Haas frequencies. The specific-heat evidence for two gaps is itself strong evidence of a second band at the Fermi surface, and the preponderance of theoretical work suggests that the e_g' surface is the most likely possibility. Penetration-depth measurements have also been interpreted in terms of two gaps,[66] and there is a recent report[67] that x-ray Compton scattering measurements show the presence of the e_g' pockets directly. The evidence for the existence of the e_g' pockets raises the question of why, if they really exist, they are not seen in ARPES. The importance of this question has been recognized in several papers, but the only answer that seems to be consistent with all the experimental claims lies in the sensitivity of ARPES results to surface effects.[52,54,55,57,67] The analysis represented in Fig. 9 leads to the conclusion that 56% of the normal-state DOS is associated with the small-gap band, in which the superconducting-state electron pairing is assumed to be weaker. Since the electron pairing is relatively weak in the a_{1g} band,[68] it seems reasonable to identify that band as the small-gap band. However, the calculations that give $N(E_F)$ separately for the a_{1g} and e_g' bands consistently assign the larger contribution to the e_g' band.[47,51,54]

X. ORDER-PARAMETER SYMMETRY

The expected signature of nodes in the energy gap is a T^2 dependence of C_{es} for line nodes and T^3 for point nodes, and comparisons of C_{es} with the symmetry of the OP predicted by theoretical models of the electron pairing are the usual basis for testing theoretical predictions with specific-heat results. Many different OPs, with and without gap nodes, have been predicted. Mazin and Johannes[4] noted that authors of papers on specific heat, nuclear-spin-relaxation rate, or muon-spin relaxation "agree that the low-temperature behavior of the DOS is not exponential, indicating the absence of a full gap." However, there is some reason to question that consensus (which may reflect, at least to some degree, a tendency to favor unconventional mechanisms when there is a choice). As described in Sec. VII, the T^2 term in C_{es} in sample 2 is not definitive proof of the presence of nodes (Mazin and Johannes[4] apparently recognized that possibility), and the absence of a T^2 term in sample 3 is not definitive proof of their absence. The T^2 term reported in Ref. 13, which is based on data that do not extend much lower in temperature than those for sample 2, is subject to the same uncertainty of interpretation, and other reported T^2 terms are not well enough defined by the data to be taken as definitive evidence of line nodes. Some muon-spin-resonance measurements have led to the conclusion that the Fermi surface is not fully gapped in the superconducting state.[69,70]

In most cases experimental values of T_1 are dominated at low temperature by a Korringa-type behavior associated with the same sample-dependent residual DOS that produces the $\gamma_r T$ term in C_{es}. At higher temperatures, a majority of the measurements have been interpreted in terms of a T^3 dependence, which was taken to be evidence of line nodes (see, e.g., Refs. 28 and 29). At low T, *but only at low* T, a T^3 dependence of T_1 is the equivalent of the T^2 dependence of C_{es}, which is characteristic of line nodes. In most cases the T^3 dependence is observed in a narrow region near T_c, where it can be attributed to strong-coupling effects, as suggested for the T dependence of C_{es} for sample 3 or to other effects that are well known in heavy-fermion superconductors (see, e.g., Ref. 71). There is, however, one notable exception, measurements by Zheng *et al.*,[72] on a sample of $Na_{0.26}CoO_2 \cdot 1.3H_2O$ with T_c, ~4.6 K, which show an approximately T^3 dependence to ~0.6 K, and essentially no suggestion of curvature that might be associated with a residual DOS even there. This sample is also unusual in that the Na content is below the range in which such high values of T_c usually occur. This raises the question of whether the electron concentration may be adjusted by another dopant, without a high concentration of O vacancies, which would circumvent the inevitability of high values of γ_r in samples with high T_c that was postulated in Sec. VII. Oxonium ions, which have been reported to affect the Co valence in the same way as Na ions[73] and which may occur in higher concentrations in low-Na content samples,[74] would seem to be a possibility.

Although the specific-heat results are ambiguous with respect to the existence of nodes, the pair breaking in the absence of magnetic-scattering centers rules out certain OP, e.g., s wave, including "extended" s wave. For a single-band superconductor any OP without a sign change would be ruled out, but for a multiband superconductor the situation is more complicated, nonmagnetic scattering can be pair breaking, depending on the interband and intraband scattering rates and pairing potentials.[75] Bang *et al.*[30] considered the effect of impurity scattering on T_1 for both $d_{x2-y2}+id_{xy}$ and d_{x2-y2} OPs, with both unitary and Born-limit scatterings. The $d_{x2-y2}+id_{xy}$ OP, for which there are no gap nodes, gives the observed residual DOS just as well as the d_{x2-y2} OP, for which there are nodes. With unitary scattering it gives the best overall agreement with the T_1 data, and, of the four cases considered, it is the only one that gives a superconducting-state DOS that is qualitatively consistent with the specific-heat results for samples 2 and 3. Thus, among the many OPs that have been suggested, $d_{x2-y2}+id_{xy}$, for which there are no nodes in the gap, is more consistent with the specific heat and with T_1 results than d_{x2-y2}. It has

also been suggested on the basis of a *t-J* model on a triangular lattice.[76–78]

XI. SUMMARY

$Na_{0.3}CoO_2 \cdot 1.3H_2O$ is another example of two-band two-gap superconductivity. The sample dependence of its properties is a consequence of a nonmagnetic pair-breaking action that increases with sample age, ultimately weakening the electron pairing in the superconducting state to the point that superconductivity gives way to a competing order. In the superconducting state the pair breaking produces an increasing residual density of states and acts preferentially in the electron band with the smaller gap to change the nature of the superconducting condensate by shifting the relative contributions of the two electron bands. The changes in the specific heat are consistent with other recent reports of the effects of sample age, including an increase in the concentration of O vacancies. Identification of the O vacancies as the pair-breaking centers provides a consistent understanding of all the effects of sample age and suggests unusual competing roles for the O vacancies—tuning the carrier concentration to increase T_c at low concentrations and destroying superconductivity by pair breaking at high concentrations. The onset of the transition to the mixed state is independent of applied magnetic field, suggesting the presence of strong fluctuation effects.

The presence of two gaps is, by itself, evidence for the existence of a second electron band at the Fermi surface, presumably the six e_g' hole pockets that appear in some, but not all, band-structure calculations. In addition, the normal-state density of states derived from the specific-heat results is in reasonable agreement with band-structure calculations only if the e_g' pockets are present, as well as the well established a_{1g} surface.

The specific-heat results do not give unambiguous evidence for either the presence or absence of nodes in the energy gap. However, the nonmagnetic pair breaking does impose significant constraints on the nature of the order parameter, even though they are more complicated for a two-band superconductor than for a single-band superconductor.

ACKNOWLEDGMENTS

We thank B. H. Brandow, D.-H. Lee, I. I. Mazin, D. J. Singh, P. Zhang, V. Kresin, and R. E. Walstedt for helpful comments and discussions and A. Bussman-Holder for communicating results of calculations of the specific heat of sample 3. The work at LBNL was supported by the Director, Office of Science, Office of Basic Energy Sciences, of the U.S. Department of Energy under Contract No. DE–AC02–05CH11231 and that at Princeton by NSF under Grant No. DMR-0213706 and by DOE-BES under Grant No. DE-FG02-98-ER45706. N.O. was supported, in part, by the DAAD.

[1] J. G. Bednorz and K. A. Muller, Z. Phys. B: Condens. Matter **64**, 189 (1986).
[2] A. Schilling, M. Cantoni, J. D. Guo, and H. R. Ott, Nature (London) **363**, 56 (1993).
[3] K. Takada, H. Sakurai, E. Takayama-Muromachi, F. Izumi, R. A. Dilanian, and T. Sasaki, Nature (London) **422**, 53 (2003).
[4] I. I. Mazin and M. E. Johannes, Nat. Phys. **1**, 91 (2005).
[5] G. Cao, C. Feng, Y. Xu, J. Shen, M. Fang, and Z.-a Xu, J. Phys. Condens. Matter **15**, L519 (2003).
[6] R. Jin, B. C. Sales, P. Khalifah, and D. Mandrus, arXiv:cond-mat/0306066 (unpublished).
[7] R. Jin, B. C. Sales, P. Khalifah, and D. Mandrus, Phys. Rev. Lett. **91**, 217001 (2003).
[8] B. G. Ueland, P. Schiffer, R. E. Schaak, M.-L. Foo, V. L. Miller, and R. J. Cava, Physica C **402**, 27 (2004).
[9] F. C. Chou, J. H. Cho, P. A. Lee, E. T. Abel, K. Matan, and Y. S. Lee, arXiv:cond-mat/0306659 (unpublished).
[10] F. C. Chou, J. H. Cho, P. A. Lee, E. T. Abel, K. Matan, and Y. S. Lee, Phys. Rev. Lett. **92**, 157004 (2004).
[11] B. Lorenz, J. Cmaidalka, R. L. Meng, and C. W. Chu, Physica C **402**, 106 (2004).
[12] H. D. Yang, J.-Y. Lin, C. P. Sun, Y. C. Kang, K. Takada, T. Sasaki, H. Sakurai, and E. Takayama-Muromachi, arXiv:cond-mat/0308031 (unpublished)
[13] H. D. Yang, J. Y. Lin, C. P. Sun, Y. C. Kang, C. L. Huang, K. Takada, T. Sasaki, H. Sakurai, and E. Takayama-Muromachi, Phys. Rev. B **71**, 020504(R) (2005).
[14] R. Jin, B. C. Sales, S. Li, and D. Mandrus, Phys. Rev. B **72**, 060512(R) (2005).
[15] N. Oeschler, R. A. Fisher, N. E. Phillips, J. E. Gordon, M.-L. Foo, and R. J. Cava, Physica B (Amsterdam) **359-361**, 479 (2005); Chin. J. Physiol. **43**, 574 (2005).
[16] N. Oeschler, R. A. Fisher, N. E. Phillips, J. E. Gordon, M.-L. Foo, and R. J. Cava, arXiv:cond-mat/0503690 (unpublished); Europhys. Lett. **82**, 47011 (2008).
[17] H. Fu, D.-H. Lee, N. Oeschler, R. A. Fisher, N. E. Phillips, M.-L. Foo, and R. J. Cava (unpublished).
[18] H. Ohta, C. Michioka, Y. Itoh, and K. Yoshimura, J. Phys. Soc. Jpn. **74**, 3147 (2005).
[19] P. W. Barnes, M. Avdeev, J. D. Jorgensen, D. G. Hinks, H. Claus, and S. Short, Phys. Rev. B **72**, 134515 (2005).
[20] R. E. Schaak, T. Klimczuk, M.-L. Foo, and R. J. Cava, Nature (London) **424**, 527 (2003).
[21] P. V. Hobbs, *Ice Physics* (Clarendon, Oxford, 1974).
[22] T. Sasaki, P. Badica, N. Yoneyama, K. Yamada, K. Togano, and N. Kobayashi, J. Phys. Soc. Jpn. **73**, 1131 (2004).
[23] Z. Ren, C. Feng, Z. Xu, M. Fang, and G. Cao, Phys. Rev. B **76**, 132501 (2007).
[24] J. Y. Uemura, Solid State Commun. **120**, 347 (2001).
[25] R. J. Radtke, K. Levin, H.-B. Schüttler, and M. R. Norman, Phys. Rev. B **48**, 653 (1993).
[26] L. S. Borkowski and P. J. Hirschfeld, Phys. Rev. B **49**, 15404 (1994).
[27] P. J. Hirschfeld, W. O. Putikka, and D. J. Scalapino, Phys. Rev. B

50, 10250 (1994).
[28] K. Ishida, Y. Ihara, Y. Maeno, C. Michioka, M. Kato, K. Yoshimura, K. Takada, T. Sasaki, H. Sakurai, and E. Takayama-Muromachi, J. Phys. Soc. Jpn. **72**, 3041 (2003).
[29] T. Fujimoto, G. Q. Zheng, Y. Kitaoka, R. L. Meng, J. Cmaidalka, and C. W. Chu, Phys. Rev. Lett. **92**, 047004 (2004).
[30] Y. Bang, M. J. Graf, and A. V. Balatsky, Phys. Rev. B **68**, 212504 (2003).
[31] D. K. Finnemore, D. L. Johnston, J. E. Ostenson, F. H. Spedding, and B. J. Beaudry, Phys. Rev. **137**, A550 (1965).
[32] R. A. Fisher, G. Li, J. C. Lashley, F. Bouquet, N. E. Phillips, D. G. Hinks, J. D. Jorgensen, and G. W. Crabtree, Physica C **385**, 180 (2003).
[33] K. Deguchi, Z. Q. Mao, H. Yaguchi, and Y. Maeno, Phys. Rev. Lett. **92**, 047002 (2004).
[34] M. E. Zhitomirsky and T. M. Rice, Phys. Rev. Lett. **87**, 057001 (2001).
[35] H. Padamsee, J. E. Neighbor, and C. A. Schiffman, J. Low Temp. Phys. **12**, 387 (1973).
[36] D. Sanchez, A. Junod, J. Muller, H. Berger, and F. Lévy, Physica B (Amsterdam) **204**, 167 (1995); C. L. Huang, J. Y. Lin, Y. T. Chang, C. P. Sun, H. Y. Shen, C. C. Chou, H. Berger, T. K. Lee, and H. D. Yang, Phys. Rev. B **76**, 212504 (2007).
[37] D. J. Scalapino (private communication); This result is also suggested by calculations of the density of states e.g., by P. J. Hirschfeld, P. Wölfle, and D. Einzel, Phys. Rev. B **37**, 83 (1988); and by D. J. Scalapino, Phys. Rep. **250**, 329 (1995).
[38] A. Bussmann-Holder (private communication).
[39] C. Caroli, P. G. deGennes, and J. Matricon, Phys. Lett. **9**, 307 (1964).
[40] K. Maki, Phys. Rev. **139**, A702 (1965).
[41] G. E. Volovik and N. B. Kopnin, Phys. Rev. Lett. **78**, 5028 (1997).
[42] N. Nakai, M. Ichioka, and K. Machida, J. Phys. Soc. Jpn. **71**, 23 (2002).
[43] F. Bouquet, Y. Wang, I. Sheikin, T. Plackowski, A. Junod, S. Lee, and S. Tajima, Phys. Rev. Lett. **89**, 257001 (2002).
[44] R. C. Morris, R. V. Coleman, and R. Bhandari, Phys. Rev. B **5**, 895 (1972).
[45] M. Mochizuki, H. Q. Yuan, and M. Ogata, J. Phys. Soc. Jpn. **76**, 023702 (2007).
[46] D. J. Singh, Phys. Rev. B **61**, 13397 (2000).
[47] M. D. Johannes, I. I. Mazin, D. J. Singh, and D. A. Papaconstantopoulos, Phys. Rev. Lett. **93**, 097005 (2004).
[48] M. D. Johannes and D. J. Singh, Phys. Rev. B **70**, 014507 (2004).
[49] P. Zhang, W. Luo, M. L. Cohen, and S. G. Louie, Phys. Rev. Lett. **93**, 236402 (2004).
[50] P. Zhang, W. Luo, V. H. Crespi, M. L. Cohen, and S. G. Louie, Phys. Rev. B **70**, 085108 (2004).
[51] K.-W. Lee, J. Kunes, and W. E. Pickett, Phys. Rev. B **70**, 045104 (2004).
[52] D. J. Singh and D. Kasinathan, Phys. Rev. Lett. **97**, 016404 (2006).
[53] S. Zhou, M. Gao, H. Ding, P. A. Lee, and Z. Wang, Phys. Rev. Lett. **94**, 206401 (2005).
[54] H. Ishida, M. D. Johannes, and A. Liebsch, Phys. Rev. Lett. **94**, 196401 (2005).
[55] M. D. Johannnes, D. A. Papaconstantopoulos, D. J. Singh, and M. J. Mehl, Europhys. Lett. **68**, 433 (2004).
[56] L.-J. Zou, J.-L. Wang, and Z. Zeng, Phys. Rev. B **69**, 132505 (2004).
[57] A. Liebsch and H. Ishida, arXiv:0705.3627 (unpublished).
[58] M. Z. Hasan, Y. D. Chuang, D. Qian, Y. W. Li, Y. Kong, A. P. Kuprin, A. V. Fedorov, R. Kimmerling, E. Rotenberg, K. Rossnagel, Z. Hussain, H. Koh, N. S. Rogado, M. L. Foo, and R. J. Cava, Phys. Rev. Lett. **92**, 246402 (2004).
[59] H.-B. Yang, S.-C. Wang, A. K. P. Sekharan, H. Matsui, S. Souma, T. Sato, T. Takahashi, T. Takeuchi, J. C. Campuzano, R. Jin, B. C. Sales, D. Mandrus, Z. Wang, and H. Ding, Phys. Rev. Lett. **92**, 246403 (2004).
[60] H.-B. Yang, Z.-H. Pan, A. K. P. Sekharan, T. Sato, S. Souma, T. Takahashi, R. Jin, B. C. Sales, D. Mandrus, A. V. Fedorov, Z. Wang, and H. Ding, Phys. Rev. Lett. **95**, 146401 (2005).
[61] D. Qian, D. Hsieh, L. Wray, Y. D. Chuang, A. Fedorov, D. Wu, J. L. Luo, N. L. Wang, M. Viciu, R. J. Cava, and M. Z. Hasan, Phys. Rev. Lett. **96**, 216405 (2006).
[62] D. Qian, L. Wray, D. Hsieh, L. Viciu, R. J. Cava, J. L. Luo, D. Wu, N. L. Wang, and M. Z. Hasan, Phys. Rev. Lett. **97**, 186405 (2006).
[63] T. Shimojima, K. Ishizaka, S. Tsuda, T. Kiss, T. Yokoya, A. Chainani, S. Shin, P. Badica, K. Yamada, and K. Togano, Phys. Rev. Lett. **97**, 267003 (2006).
[64] L. Balicas, M. Abdel-Jawad, N. E. Hussey, F. C. Chou, and P. A. Lee, Phys. Rev. Lett. **94**, 236402 (2005).
[65] L. Balicas, J. G. Analytis, Y. J. Jo, K. Storr, H. Zandbergen, Y. Xin, N. E. Hussey, F. C. Chou, and P. A. Lee, Phys. Rev. Lett. **97**, 126401 (2006).
[66] H. Q. Yuan, M. B. Salamon, and D. Vandervelde, Bull. Am. Phys. Soc. **50**(1), 929 (2005).
[67] J. Laverock, S. B. Dugdale, J. A. Duffy, J. Wooldridge, G. Balakrishnan, M. R. Lees, G.-q. Zheng, D. Chen, C. T. Lin, A. Andrejczuk, M. Itou, and Y. Sakurai, Phys. Rev. B **76**, 052509 (2007).
[68] D.-H. Lee (private communication).
[69] A. Kanigel, A. Keren, L. Patlagan, K. B. Chashka, P. King, and A. Amato, Phys. Rev. Lett. **92**, 257007 (2004).
[70] W. Higemoto, K. Ohishi, A. Koda, S. R. Saha, R. Kadono, K. Ishida, K. Takada, H. Sakurai, E. Takayama-Muromachi, and T. Sasaki, Phys. Rev. B **70**, 134508 (2004).
[71] R. H. Heffner and M. R. Norman, Comments Condens. Matter Phys. **17**, 361 (1996); arXiv:cond-mat/9506043 (unpublished).
[72] G.-q. Zheng, K. Matano, R. I. Meng, J. Cmaidalka, and C. W. Chu, J. Phys.: Condens. Matter **18**, L63 (2006).
[73] K. Takada, K. Fukuda, M. Osada, I. Nakai, F. Izumi, R. A. Dilanian, K. Kato, M. Takata, H. Sakurai, E. Takayama-Muromachi, and T. Sasaki, J. Mater. Chem. **14**, 1448 (2004).
[74] C. J. Milne, D. N. Argyriou, A. Chemseddine, N. Aliouane, J. Veira, S. Landsgesell, and D. Alber, Phys. Rev. Lett. **93**, 247007 (2004).
[75] A. A. Golubov and I. I. Mazin, Phys. Rev. B **55**, 15146 (1997).
[76] G. Baskaran, Phys. Rev. Lett. **91**, 097003 (2003).
[77] M. Ogata, J. Phys. Soc. Jpn. **72**, 1839 (2003).
[78] Q.-H. Wang, D.-H. Lee, and P. A. Lee, Phys. Rev. B **69**, 092504 (2004).